Preparation of silica/silver (I) and silica/mercury (II) heterogeneous composite particles **via** 3-(mercaptopropyl)triethoxysilane

Hayder H. AL-Hmedawi , Suhad K. Abass , Mohammed T. Khathi

ABSTRACT: The heterogeneous composite particles MPTESH-Ag , MPTESH-Ag-OH and MPTESH-Hg-OH has been prepared in the presence of mercaptopropyltriethoxysilane (MPTES) and metals ion Ag+ and Hg2+ in neutral and basic medium. The prepared complexes are not dissolved of any common solvents, this conform heterogeneous nature of these compounds. The complexes are characterized by different techniques, X-ray diffraction technique showed that the MPTES-Ag has amorphous face, while the MPTES-Ag-OH and MPTES-Hg-OH have crystalline face .The atomic force microscope (AFM) technique was proved that the prepared compound have spherical nano particles. The N2-adsorption-desorption technique showed the BET surface area, total pore volume and pore diameter of these complexes .

Keywords: Heterogeneous composite particles, mercaptopropyltriethoxysilane, silver, mercury.

1. INTRODUCTION

The synthesis of hybrid organic/inorganic mesoporous materials is a field of expanding interest, due to the potential applications of these materials in a variety of processes, covering catalysis, adsorption and nanotechnology[1]. In recent years, many preparation routes [2–5], by which metal nanoparticles are immobilized onto the various inorganic supports, have been developed by many scientists to expand the application area and to control the morphology and the behavior of nano-materials. These composite particles with hollow structure by novel strategy including water-in-oil (W/O) emulsion and polyol process.

via 3-mercaptopropyltrimethoxysilane (MPTMS)-functionalized hollowsilica particles with tetraethyl orthosilicate (TEOS) and MPTMS successively into W/O emulsion. These hollow particles were coated with silver nanoparticles through polyol process[13]. Thiol-functionalized silicas applied to the removal of

materials have greatly potential application in various fields such as surface enhanced Raman scattering (SERS) [6], photonic crystals [7], catalysis [8], and biochemistry for chemical sensors [9] and antibacterial materials [10], etc. Especially, silver-supported silica materials, such as silica glass [11] and silica thin films [12], are expected to be good candidates for antibacterial materials due to their good chemical durability and high antibacterial activity. Jong-Min Lee et.al have been prepared Silica/silver heterogeneous composite

Hg(II) from aqueous solutions were first prepared as amorphous porous adsorbents [14–17]. The effect of pH on the adsorption of Hg(II) species by thiol-functionalized mesoporous silicas have been prapared with respect to the accessibility to the active centers and to the selectivity of the binding process in the presence of other metal ions interferences[18]. In the present work ,we prepared hybrid organic/inorganic mesoporous materials derived from 3-(mercaptopropyl)triethoxysilane and silver ,mercury ions in neutral and basic medium.

Hayder H. AL-Hmedawi is currently pursuing Dr in science in inorganic chemistry in Karbala University , Iraq .E-mail : hayderalhmedawy@gmail.com

.

Suhad K. Abass is currently pursuing Dr in science in inorganic chemistry in Karbala University , Iraq .E-mail : ad-suh@yahoo.com

Mohammed T. Khathi is currently pursuing Dr in science in inorganic chemistry in Karbala University , Iraq .E-mail : dr.mohammedturki@yahoo.com

2.*EXPERIMENTAL*

2.1 Chemicals

3(mercaptopropyl)triethoxysilane(MPTES)(Sigma–Aldrich,95%),Ethanol(absolute), (BDH,>99%), potassium hydroxide (Fluka, 99%),silver nitrate(Fluka, 99%), mercury chloride($HgCl_2$), were each used without further purification.

2.2 Characterization

Powder X-ray diffraction of the complexes were collected from (stoe,stidy-mp)University of kashan-Iran, nitrogen adsorption porosimetry (nova2000,quantachrome) at University of Tehran Iran,the samples were out gassed for about 12 h at 105 ºC under vacuum at 10^{-3} mm Hg in the degassing port of the adsorption analyzer, the specific surface area of the prepared complex were calculated using the BET model. Infrared spectra were obtained by KBr disc

over the wavenumber range of 4000–400 cm^{-1} using (FTIR–8400S Shimadzu). The three dimensional (AFM) images for the prepared complexes was obtained using CSPM-AA3000.

2.3.Synthesis

10 mmole of 3-Mercaptopropyltriethoxysilane (MPTES) was mixed with 10 mL of ethanol absolute and 10 mmol of appropriate salt ($AgNO_3$ or $HgCl_2$) was dissolved in 10 mL of water(silver complexes prepared in neural medium and basic medium). MPTES solution and metal salt solution were mixed and refluxed for 30 minutes. The final product was filtered and washed with cold methanol several times and lastly dried at 45 ºC for 5 hours, the complexes have been labeled are MPTES-Ag, MPTES-Ag-OH and MPTES-Hg-OH respectively . The complexes was non soluble in any solvents. Physical properties of the complex is shown in Table(2-1).

3.RESULTS AND DISCUSSION

Table (1): Shows the physical data for the new complexes. The new complexes have higher melting points and cannot dissolve in any common solvents. These results indicate that complexes as a dimers contain the siloxane (Si–O–Si) and silanol (Si–OH) groups .

Table (3-1): Physical data for prepared complexes.

Complex	m.p°	solvent					Nitrogen adsorption			Average particle size(nm)
		Ethanol	methanol	DMF	DMSO	Acetone	BET surface area ($m^2 g^{-1}$)	Total pore volume ($cm^3 g^{-1}$)	Pore diameter (A°)	
MPTES-Ag	>300 °C	-	-	-	-	-	5.813	0.008	24.69	84.11
MPTES-Ag-OH	> 300 °C	-	-	-	-	-	23.898	0.041	16.88	86.83
MPTES-Hg-OH	> 300 °C	-	-	-	-	-	51.129	0.095	19.28	97.91

3.2. X-ray diffraction

Figures 1-3 shows x-ray diffraction for prepared complexes, figure 1. shows the X-ray diffraction of the complex MPTES-Ag . The X-ray diffraction pattern of MPTES-Ag Fig.1, indicated the absence of any ordered crystalline structure., i.e. a broad peak centered at 2θ angle of around 25° which confirmed the amorphous nature of the sample. The X-ray diffraction pattern of MPTES-Ag-OH Fig.2 indicated ordered crystalline structures of this complex. Major peaks in this figure at °2θ = 22.195, 27.460, 27.785 , 34.365 , 37.870 , 39.365 , 48.255, 49.070 , 51.810 , 54.810 ,84.775. Figure(3) shows X-ray diffraction pattern of MPTES-Hg-OH .Major peaks in this figure at °2θ = 33.090, 47.420,59.130, 69.460,79.070, 88.380, these peaks indicated ordered crystalline structures of this complex.

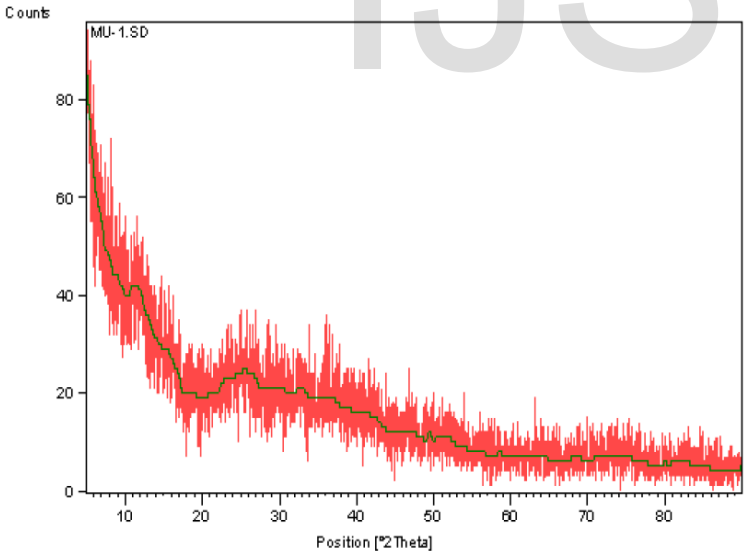

Figure(1).X-ray spectrum of MPTES-Ag

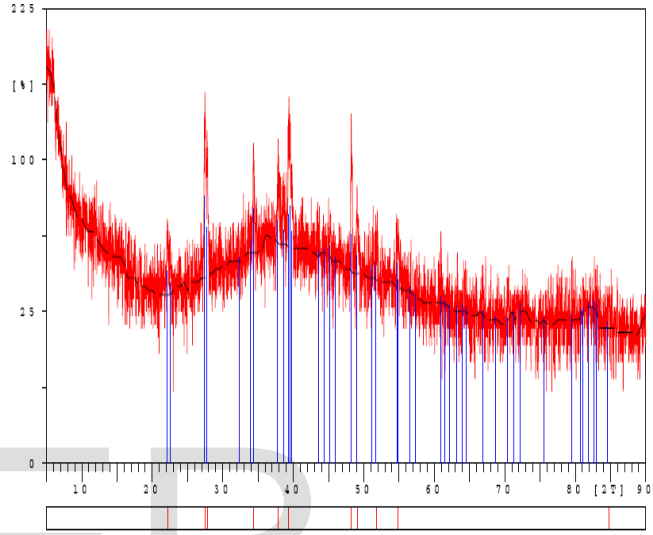

Figure(2).X-ray spectrum of MPTES-Ag-OH

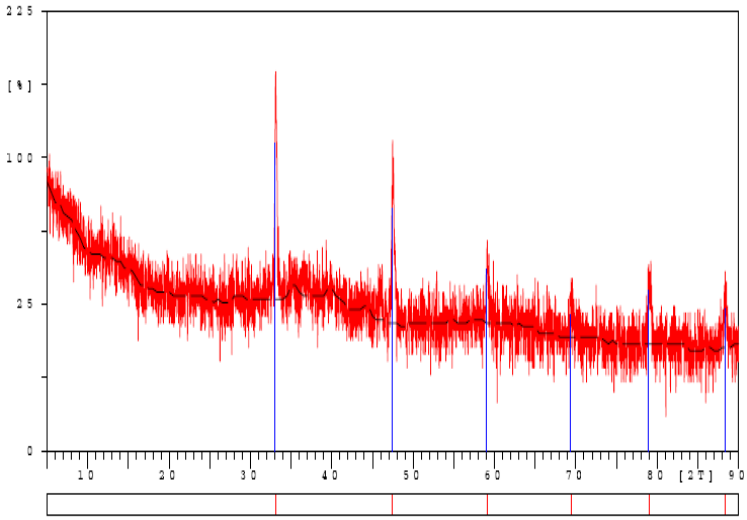

Figure(3).X-ray spectrum of MPTES- Hg-OH

ISSN 2229-5518

3.2 IR spectra

The FT-IR spectrum of the complexes (Fig.5-7) showed the bands around 1110 and 670 cm^{-1}, which assigned to siloxane (Si–O–Si) vibration modes [19]. The band at 1650 cm^{-1} could be due to physically/ chemically absorbed water on the surface and the band around 3415 cm^{-1} can be due to the silanol (–OH) group on the silicon atom [20]. From observation spectrum of MPTES Fig. (4) , the bands which explained of complexes MPTES-Ag , MPTES-AgOH and MPTES-Hg-OH it not found in the MPTES.

The broad bands around 1400 cm^{-1} were assigned to the C–H bending vibrations of the CH_2 in complexes ,while these bands appeared in MPTES as a two peak at 1444 cm^{-1} and 1390 cm^{-1} were assigned to the C–H bending symmetrical and asymmetrical vibrations of the CH_2 [21] . A band around 450cm^{-1} can be assigned to the S–M bond . These results clearly indicate that MPTES successful complications with Ag^{+} and Hg^{+2}.

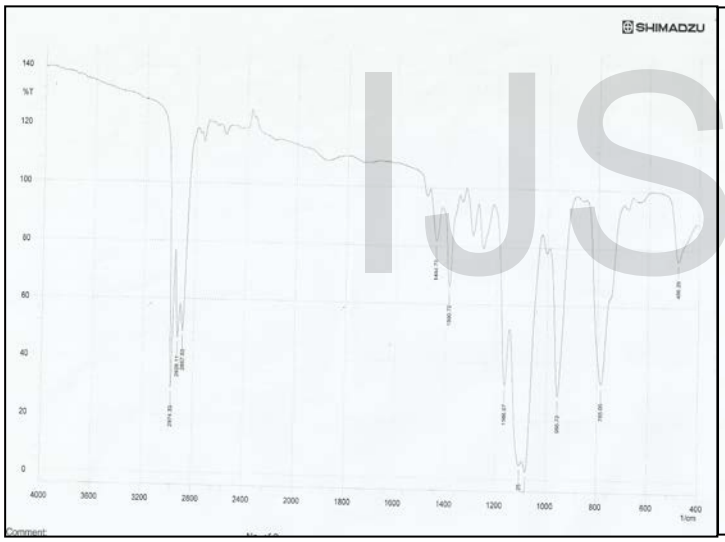

Figure (4).FTIR spectrum of MPTES

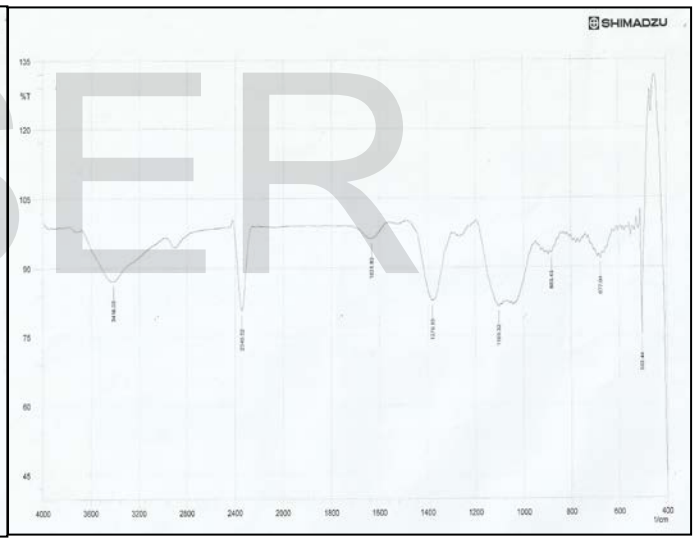

Figure(5).FTIR spectrum of MPTES–Ag

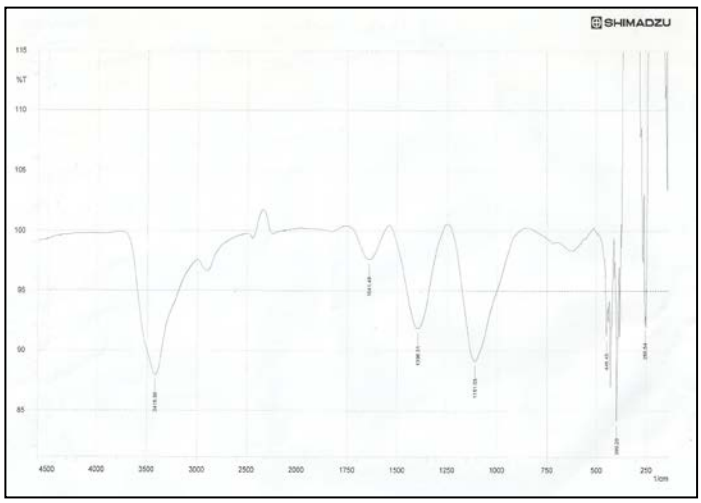

Figure(6).FTIR spectrum of MPTES- Ag-OH

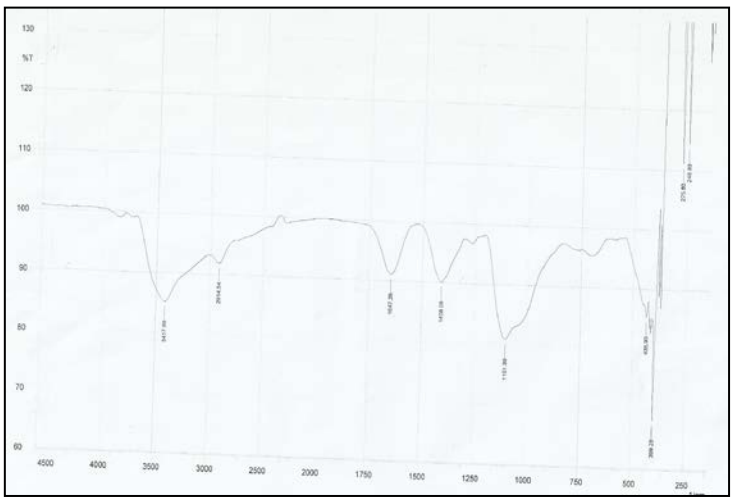

Figure(7).FTIR spectrum of MPTES Hg-OH

3.3. The nitrogen adsorption analysis

The BET analysis showed that the specific surface area of MPTES-Ag was 5.992 m^2g^{-1}. The nitrogen adsorption isotherm (Fig.8) obtained for MPTES-Ag gave a hysteresis loop observed in the range of 0.02 < *P/Po* < 1.0; this is associated with capillary condensation according to IUPAC classification. The isotherm shown is of type IV and exhibited an H4 hysteresis loop [129]. MPTES-Ag have a very sharp distribution at a radius of around 5 nm, indicates the presence of uniform sized pores [146].

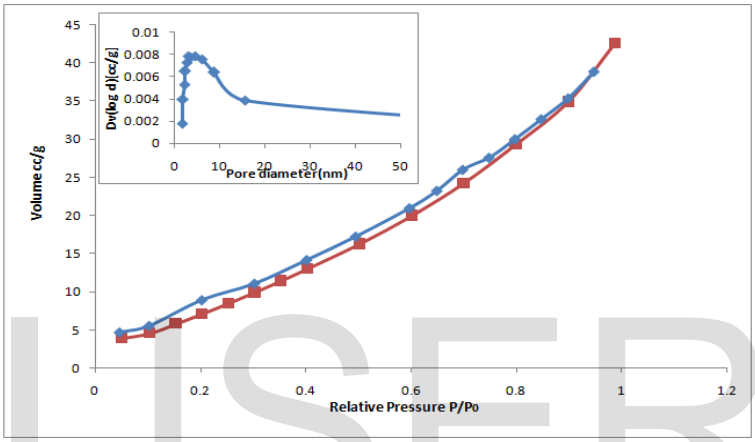

Fig.8: The nitrogen adsorption–desorption isotherms of MPTES-Ag. The inset shows the corresponding pore size distribution.

The specific surface area of MPTES-Ag-OH was found to be 23.89 m^2g^{-1} (Table 1). The nitrogen adsorption isotherm obtained for MPTES-Ag-OH (Fig. 9) gave a hysteresis loop observed in the range of 0.02 < *P/Po* < 1.0; this is associated with capillary condensation according to IUPAC classification. The isotherm shown is of type IV and exhibited an H3 hysteresis loop [22]. MPTES-Ag-OH had a broad distribution at a radius of around 5 nm which fall in the mesoporous range [23].

The specific surface area of MPTES-Hg-OH was found to be 51.12m^2g^{-1} (Table 1). The nitrogen adsorption isotherm obtained for MPTES-Hg-OH (Fig. 10) gave a hysteresis loop observed in the range of 0.02 < *P/Po* < 1.0; this is associated with capillary condensation according to IUPAC classification. The isotherm shown is of type IV and exhibited an H3 hysteresis loop [22]. MPTES-Ag-OH had a broad distribution at a radius of around 9 nm which fall in the mesoporous range [23].

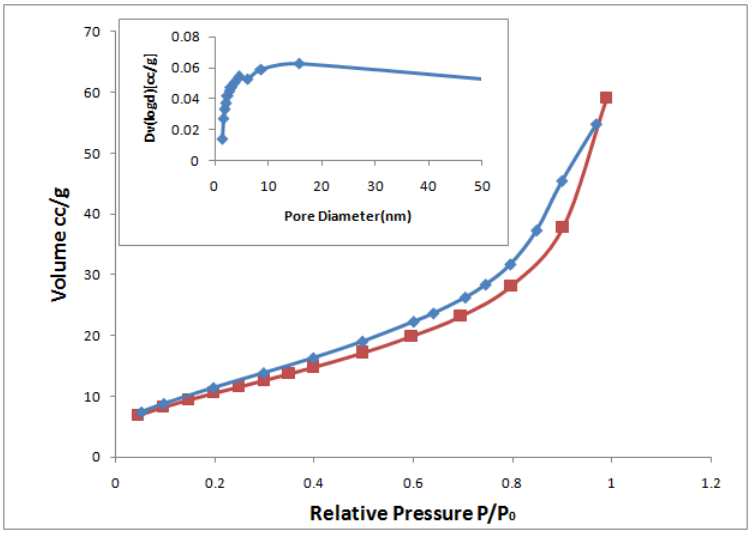

Fig.10: The nitrogen adsorption–desorption isotherms of MPTES-Hg-OH. The inset shows the corresponding pore size distribution.

3.4.Atomic force microscopy (AFM)

The atomic force microscopy (AFM) images and granularity normal distribution of the MPTES-Ag are shown in Fig. 11 and Fig. 12. The grain structure of MPTES-Ag look like spherical with high roughness of the surface. The structures and size distribution is shown in the images, the particles size in diameter was to be 84.11 nm.

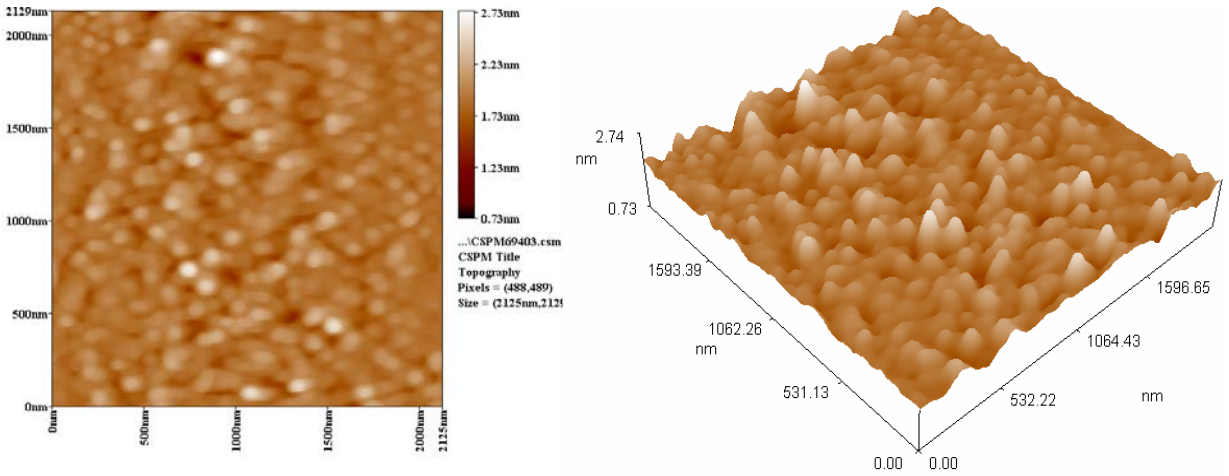

Fig. 11: Three-dimensional AFM images for MPTES-Ag.

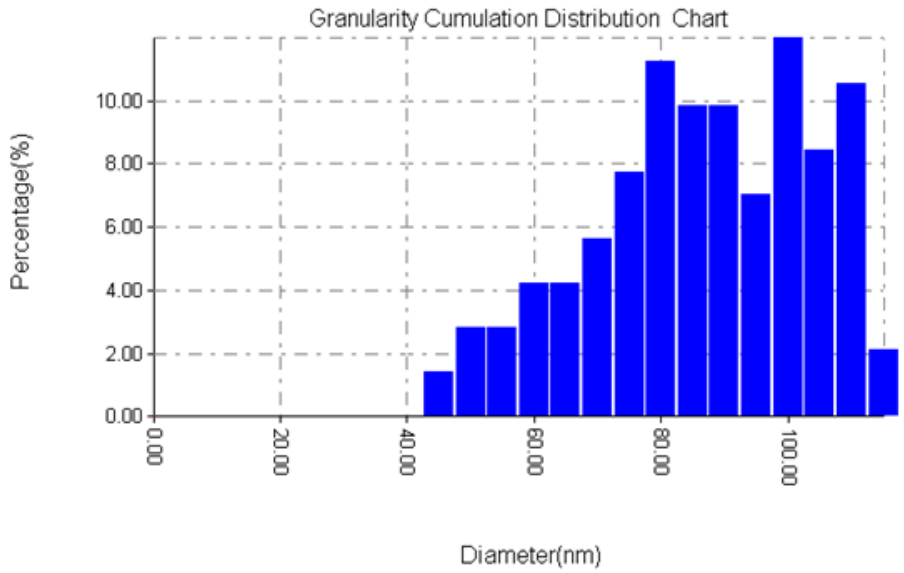

Fig.12: Granularity normal distribution chart of MPTES-Ag

The atomic force microscopy (AFM) images of the MPTES-Ag-OH are shown in Fig. 13. From these images the MPTES-Ag-OH has an average particle size of 86.83 nm as shown in the granularity normal distribution chart (Fig.14). The structures and size distribution is shown in the images, the sticks between particles was also shown.

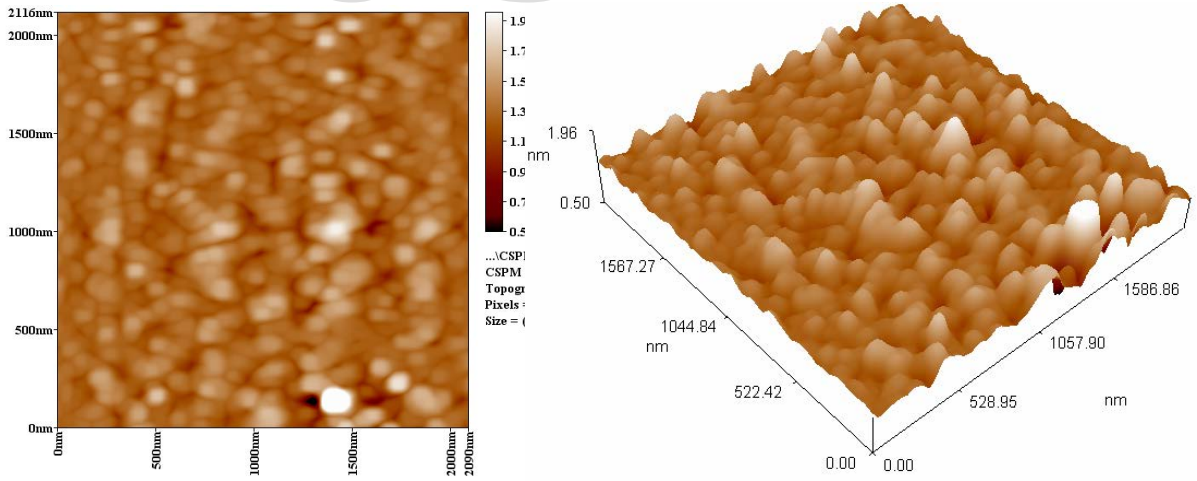

Fig. 13: Three-dimensional AFM images for MPTES-Ag-OH.

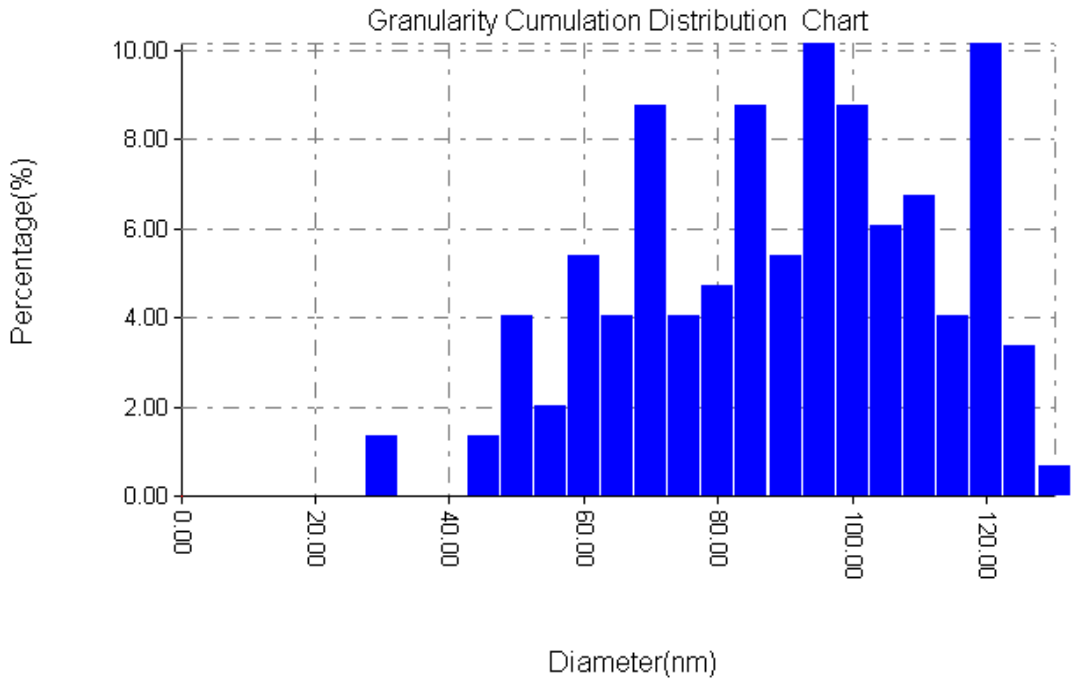

Fig.14: Granularity normal distribution chart of MPTES-Ag-OH

The dense packing of the MPTES-Hg-OH particles was illustrated by AFM. In the Fig. 15, the AFM of the material showed MPTES-Hg-OH particles were packed tightly three dimensionally. The morphology of the catalyst shows two types of the surface, large and small end. From these images (Fig. 15 and Fig. 16), the MPTES-Hg-OH has an average particle size of large end is 97.91 nm as shown by granularity normal distribution chart

.

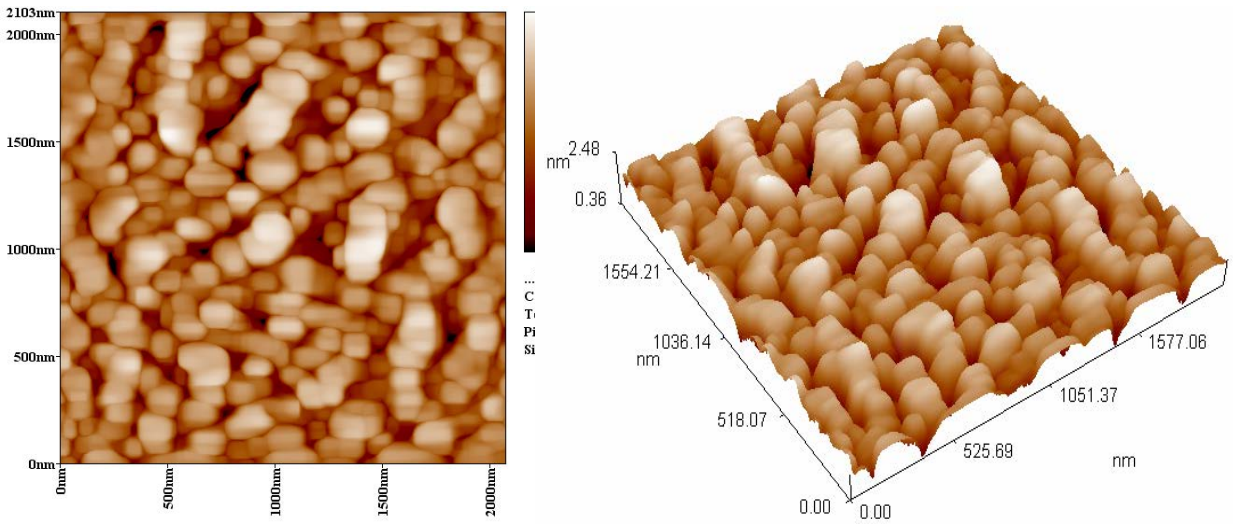

Fig. 15: Three-dimensional AFM images for MPTES-Hg-OH.

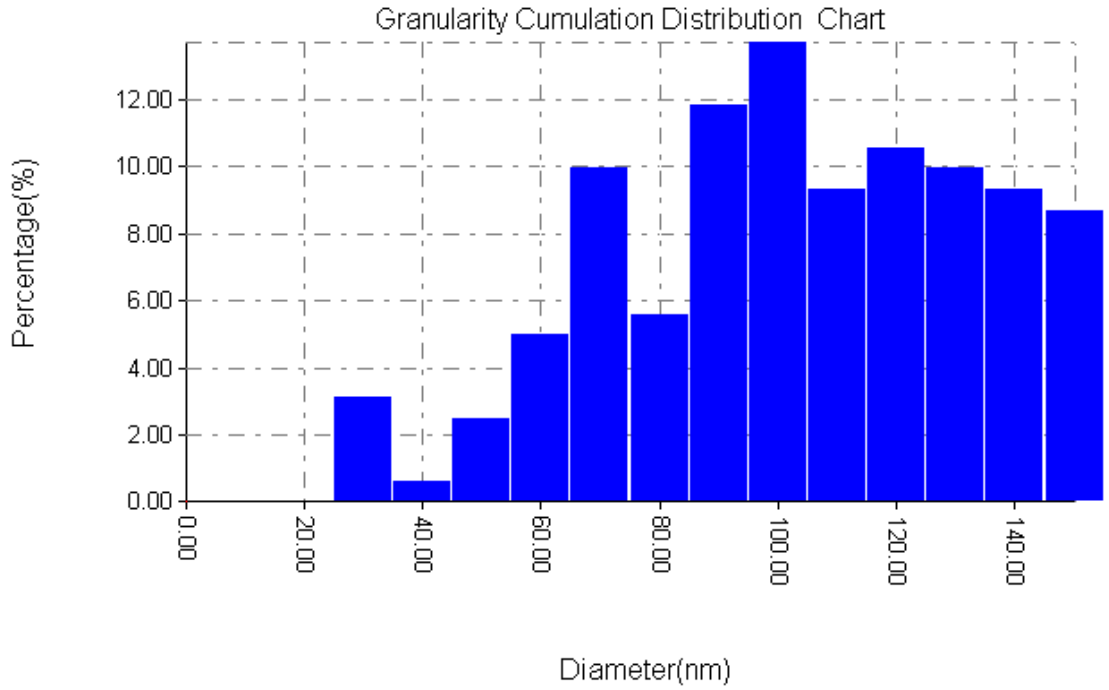

Fig.16: Granularity normal distribution chart of MPTES-Hg-OH

4. CONCLUSIONS

According to results obtained from physical techniques above and the not solubility of these de that these complexes as a dimers as a hybrid organic-inorganic materials as suggested fellow :

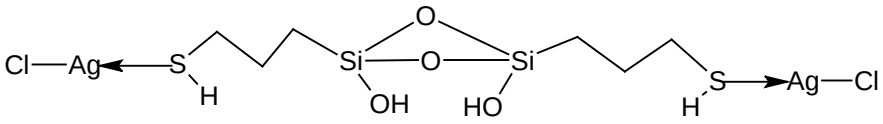

MPTES-Ag

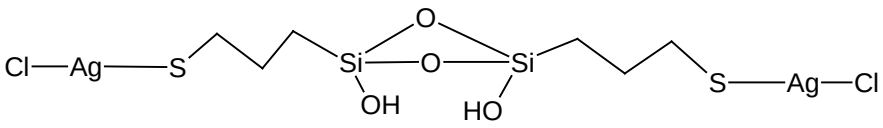

MPTES-Ag-OH

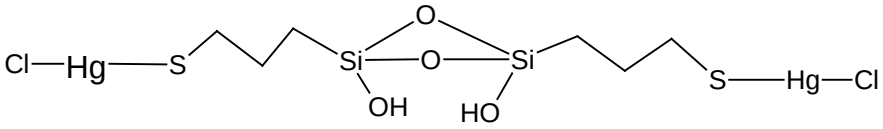

MPTES-Hg-OH

6. REFERENCES

1. C.Sanchez, B.Julia´n, P. Belleville and M. Popall, Mater. Chem., 15(2005) 3559 .

2. D. Lawless, S. Kapoor, P.Kennepohl, D. Meisel, N. Serpone, J. Phys. Chem. 98 (1994) 9619.
3. S.J. Oldenburg, R.D. Averitt, S.L. Westcott, N.J. Halas, Chem. Phys. Lett. 288 (1998) 243.
4. Y. Kobayashi, V. Salgueiri˜no-Maceira, L.M. Liz-Marz´an, Chem. Mater. 13 (2001) 1630.
5. W. Wang, S.A. Asher, J. Am. Chem. Soc. 123 (2001) 12528.
6. S. Nie, S.R. Emory, Science 275 (1997) 1102.
7. Z.L. Wang, C.T. Chan, W.Y. Zhang, Z. Chen, N.B. Ming, P. Sheng, Phys. Rev. B 64 (2001) 113108.
8. C.W. Chen, T. Serizawa, M. Akashi, Chem. Mater. 11 (1999) 1381.
9. S.A. Kalele, S.S. Ashtaputre, N.Y. Hebalkar, S.W. Gosavi, D.N. Deobagkar, D.D. Deobagkar, S.K. Kulkarni, Chem. Phys. Lett. 404 (2005) 136.
10. J.X.Wang, L.X.Wen, Z.H.Wang, J.F. Chen, Mater. Chem. Phys. 96 (2006)90.
11. M. Kawashita, S. Tsuneyama, F. Miyaji, T. Kokubo, H. Kozuka, K.Yamamoto, Biomaterials 21 (2000) 393.
12. H.J. Jeon, S.C. Yi, S.G. Oh, Biomaterials 24 (2003) 4921.
13. Jong-Min Lee, Yong-Geun Lee, Dae-Wook Kim, Chul Oh, Sang-Man Koo, Seong-Geun Oh, Colloids and Surfaces A: Physicochem. Eng. Aspects 301 (2007) 48–54.
14. U. Koklu, Chim. Acta Turc. 12 (1984) 265.
15. A.R. Cestari, C. Airoldi, J. Braz. Chem. Soc. 6 (1995) 291.
16. E.F.S. Vieira, J. De, A. Simoni, C. Airoldi, J. Mater. Chem. 7 (1997)2249.
17. A.R. Cestari, C. Airoldi, J. Coll. Interf. Sci. 195 (1997) 338.
18. A. Walcarius∗, Cyril Delacˆote, Analytica Chimica Acta 547 (2005) 3–13
19. X. J .Xiang, J. W.Qian, , W. Y.Yang, , M. H. Fang, , and X. Q. Qian, J. Appl. Polymer Sci., 100 (2006) 4333-4337.
20. N.Jyotiprakash, and B. Japes, J. of Metals, Materials and Minerals, 19(2009), 15-19.
21. , R.M.Silverstein, G.C.Bassler, and T.C.Marrill, ,. "Spectrometric identification of organic chemistry", John wiley and Sons., (1981) pp.72-108.
22. M.Thommes, Chem. Ing. Tech., 82(2010)1059–1073.
23. T.Takei, , O.Houshito, , Y.Yonesaki, , N.Kumada, , and N.Kinomura, J. Solid State Chem. 180(2007) 1180–1187.